

## MODIFIED ALADDIN LATTICE N30

S. Kramer and Y. Cho

The present Aladdin lattice, hereafter referred to as Synch lattice, was designed to provide nearly equal beam size in all the dipole magnets. By offsetting the quadrupole doublets after the dipoles, access to the photon beam lines was made more convenient, but destroys the symmetry of the element placement. The lattice functions for the Synch lattice are shown in Figure 1. The common bussing of the quadrupole doublets and the triplets make the Twiss functions asymmetric through the long straight section and a large negative dispersion in this region. The large value of dispersion around the period, although not by itself bad, limits the natural emittance of this lattice and makes resonance corrections difficult without influencing the chromatic properties of this lattice.

Linear Lattice Properties

Yang Cho, Ed Crosbie and Steve Kramer each attempted to adjust the lattice tune in order to reduce the dispersion in this lattice. This is easily achieved by making the phase advance  $120^\circ$  through a single dipole section. However, the beam sizes in the dipole magnets are no longer equal. The solution to this problem can be achieved by separating the bussed quadrupole and powering them separately. One such solution was proposed by Yang Cho to separate the first doublet (after the long straight section) from those in the bending section. In addition, to provide for some adjustment of the tune, two of the triplet quadrupoles were separated from each other. This proposed lattice, called the N30 lattice (for November 30th 1984 tune), is presented in Figure 2. A comparison of the linear and first order parameters for the N30 and Synch lattices are presented in Table I.

The N30 lattice shows considerably more symmetry between the beam size in the dipoles than the Synch lattice. In fact, except for the injection straight section, the lattice functions are nearly equal in all similar elements. This property should improve the higher order properties of this

lattice, since the  $\beta$  and  $\eta$  functions in the sextupoles should contribute less to the higher order resonances. Figure 3(a) shows the working point diagram for the N30 tune. The dashed lines show the second and third order resonances and fourth order resonances are shown with a dotted line. The working point is plotted for a  $\pm 1\%$  momentum change. The total tune variation is less than 0.007 in the horizontal and vertical and is shown in Fig. 3(b) in more detail.

Figure 4(a) shows the variation of the Twiss parameters<sup>1</sup> in the long straight section as a function of momentum, since  $\eta = 0$  at this point it isn't plotted. Figure 4(b) shows the ratio of the beta function for the entire period for a momentum change of 1%. As expected, the tunes and Twiss parameters have little variation with momentum. Figure 5 presents the RMS orbit distortions as calculated by the program PARTIS.<sup>2</sup> The sensitivity of this lattice to errors has improved a factor of 2 to 3 over the Synch lattice.

### Dynamic Aperture

The dynamic aperture was determined by running the tracking programs PATRIS<sup>2</sup> and PATRICIA 84.9.<sup>3</sup> Particles were considered stable if they survived a 1000 turns with a transverse position criteria of  $|x| < 1$  meter and  $|y| < 1$  meter at the sextupoles in the lattice. The starting betatron amplitude was varied in units of the natural rms beam size  $\sigma_x = \sqrt{\beta_x \epsilon_0}$  and  $\sigma_y = \sqrt{\beta_y \epsilon_0}$  where  $\epsilon_0$  = the natural emittance in the horizontal with zero coupling. The initial particle coordinates were  $(x, x') = (N_x \sigma_x, 0)$  and  $(y, y') = (N_y \sigma_y, 0)$ . The  $N_x$  and  $N_y$  were increased until the maximum stable amplitude was determined to an accuracy of  $\Delta N_{x,y} < 2.5$ . This was done using the four particles tracked by the program PATRICIA 84.9,<sup>3</sup> all of which had an equal  $x$  value and  $y = y_0 + i\Delta N_y$  (for  $i = 0, 1, 2, 3$ ). The  $y_0$  value is increased until the first unstable amplitude was determined. The limit of stability is taken midway between the greatest stable amplitude and the first unstable amplitude, then  $\Delta N_y$  is reduced a factor of 2 and four new particles are tracked with amplitudes around this limit.  $\Delta N_y$  continues to be reduced by a factor of 2 each time a new stability limit is determined, until  $\Delta N_y < 2.5$ . At that point, the greatest stable amplitude observed is taken as the dynamic aperture for that  $x$  amplitude. Then the  $x$  value is incremented and a new search for a  $N_y$  limit is begun. This search procedure continues until the desired  $N_x$  range has been scanned. This search procedure, although time

consuming, insures that all amplitudes less than the  $N_y$  are stable and not that the first stable island was found. The latter might be determined if the algorithm started at large values of  $y$  and stopped at the first stable amplitude, a procedure which would be less time consuming.

Figure 6 shows the dynamic aperture for  $\delta p/p = 0$  and  $\frac{\delta p}{p} = \pm 0.6\%$ . Also shown is the dynamic aperture for synchrotron oscillations with an initial  $\delta p/p = 0.6\%$  and phase error of zero. Beyond  $N_x = 35$ , there is no dynamic aperture even for  $N_y = 0$  and  $\delta p/p = 0$ . Figure 7 shows the trajectory for a particle with  $N_x = 35$ ,  $N_y = 3.5$ . The horizontal shows a typical third order resonance shape and the loss of aperture beyond  $N_x = 35$  is due to the  $3\nu_x = 16$  resonance. This is shown in Figure 8, where the horizontal tune is plotted as a function of the horizontal betatron amplitude ( $N_x$ ) while  $N_y$  and  $\delta p/p$  are held fixed. The program PATRICIA calculates the tune by Fourier analyzing the particle trajectory and the tune is taken as the dominant spectral component. An increase in vertical betatron amplitude reduces the horizontal tune slightly, such that the resonance isn't reached until a slightly higher  $N_x$  value. This effect isn't large since the tune spread also increases with  $N_y$ , but a particle with  $N_x = 38$ ,  $N_y = 20$  is stable even though one with  $N_x = 38$ ,  $N_y = 0$  is unstable. Although additional sextupoles could be added to minimize this resonance, it was felt better to raise the tune to  $\nu_x \approx 6$  in order to avoid the  $3\nu_x = 16$  and 20 resonances.

Figure 9 demonstrates the excellent chromatic properties of this lattice by showing the change in dynamic aperture with momentum. In this case, the dynamic aperture was calculated along a line  $N_x = N_y$  as  $\delta p/p$  was varied over the range  $|\delta p/p| < 1.2\%$ .

### Conclusion

The N30 lattice appears to have some major advantages over the present Aladdin lattice: 1) better natural emittance, 2) increased dynamic aperture, 3) reduced sensitivity to errors, 4) improved chromatic properties. However, the present working point of the N30 lattice could be improved to 1) minimize the effect of structure resonances and 2) increase the horizontal aperture.

References

- 1 The variation of the Twiss parameters with momentum were calculated using the CERN program MAD (version 3.06) and agree with the PATICIA calculations. MAD is the Methodical Accelerator Design program by F. Christoph Iselin, Reference Manual LEP Division Nov. 1, 1984.
- 2 PATRIS is the tracking program by A. Ruggiero private communication.
- 3 PATRICIA 84.9 is the latest tracking code generated by H. Weideman - SSRL ACD-Note No. 22, November 1984.

Table 1  
Comparison of ALADDIN Lattices

Function	ALADDIN Synch Lattice	ALADDIN N30 Lattice
$\sqrt{x}$	7.135	5.236
$\sqrt{y}$	7.095	6.281
$\xi_x$ (Chromaticity)	-10.809	-7.630
$\xi_y$ "	-19.245	-10.456
$K_2$ (SF)	-2.465	-1.982
$K_2$ (SD)	5.576	5.320
Horiz. Damping time	13.9	13.9
$\epsilon$ (natural)	164	117
$\sigma_{p/p}$ (natural)	0.059%	0.059%
$\eta_x$ (long straight)	-0.577	0
$\alpha_x$ ( " " )	-1.055	0
$\alpha_y$ ( " " )	-0.033	0
$B_x$ (max) (location)	11.68 (Q3)	7.552 (Q1)
$B_y$ (max) (location)	16.41 (Q2)	10.282 (Q2)
$B_x$ (Bend)	$2.183 \pm 0.628$	$1.469 \pm 0.006$
$B_y$ (Bend)	$2.340 \pm 0.354$	$2.205 \pm 0.053$
$\epsilon_x$ (max.) physical	101.5 (Q3)	162.2 (Q1)
$\epsilon_y$ (max.) physical	69.9 (Bend)	108.5 (Bend)
$K(QF)$	-5.300977	-5.5916950
$K(QD)$	5.480832	5.1741640
$K(Q1)$	-4.600982	-2.850929
$K(Q2)$	5.618463	4.1141180
$K(Q3) = K(Q3X)$	-4.651147	-2.0465905
$K(Q1X)$	—	-1.4831900
$K(Q2X)$	—	3.8871980
$K(QFX)$	—	-4.0516260
$K(QDX)$	—	4.9239590

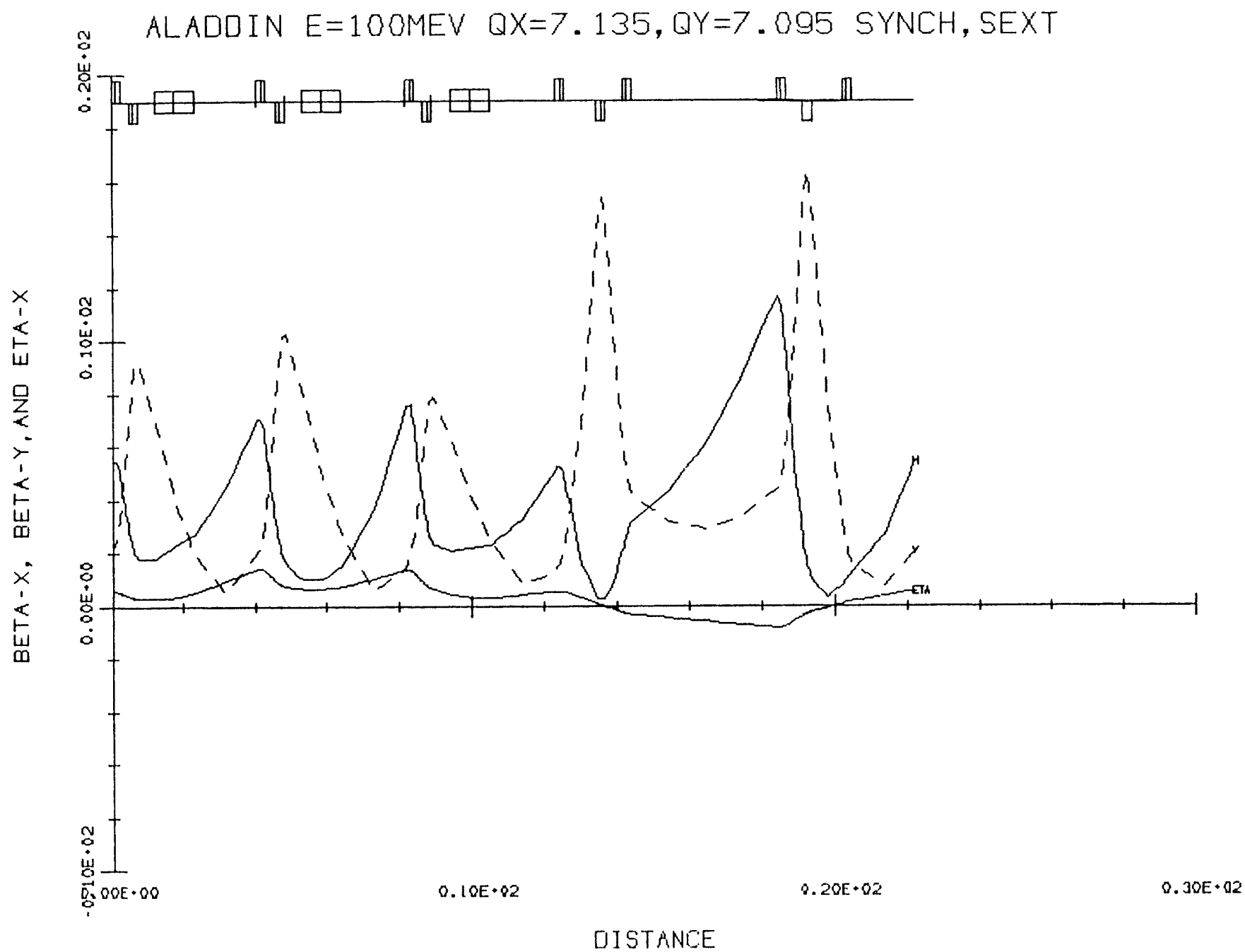


Figure 1. Aladdin "Synch" Lattice Twiss Functions

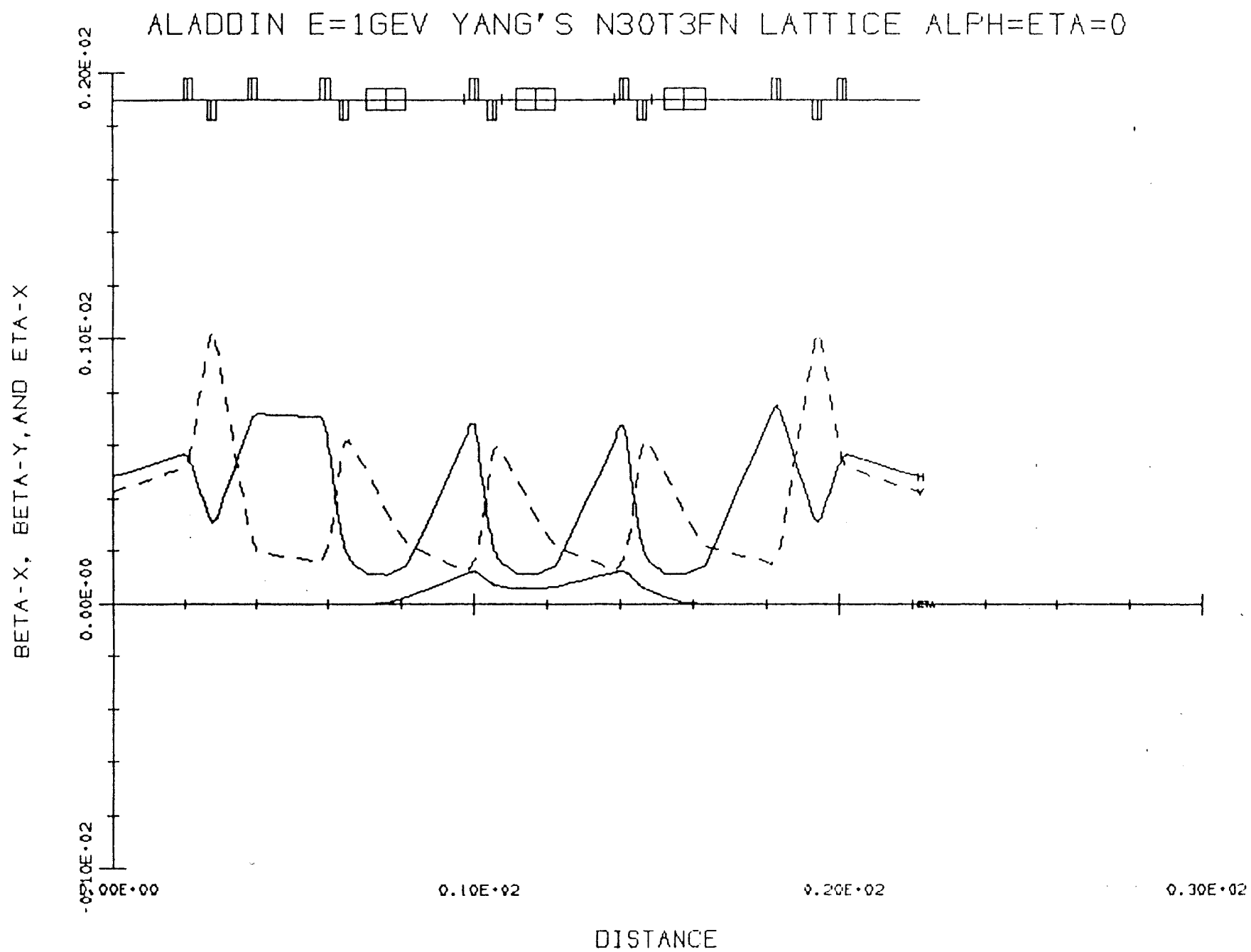


Figure 2(a). N30 Lattice Twiss Functions

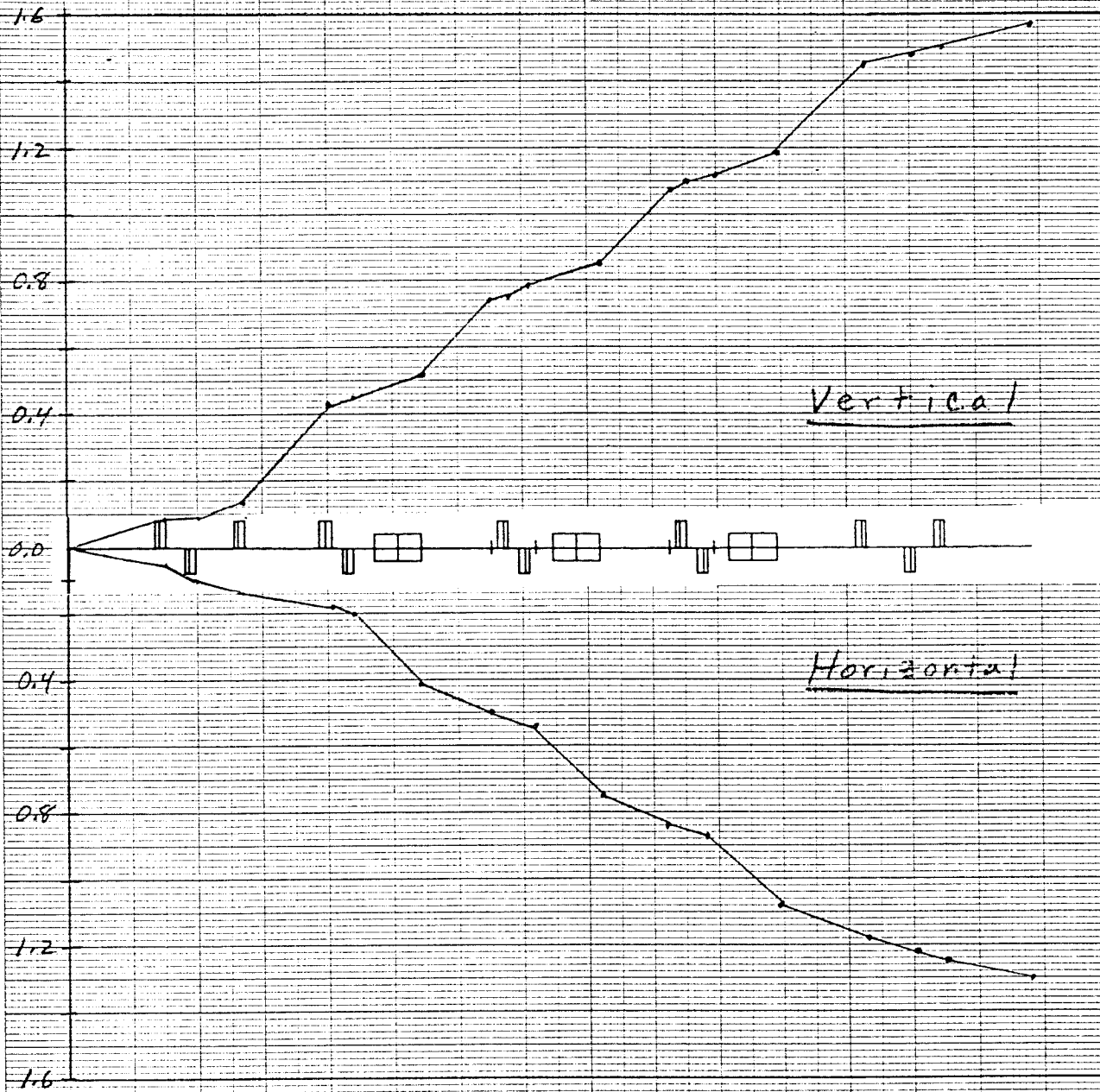
$\mu_y \text{ in } (2\pi)^{-1}$  $\mu_x \text{ in } (2\pi)^{-1}$ 

Figure 2(b). Betatron Phase Advance for N30 Lattice.



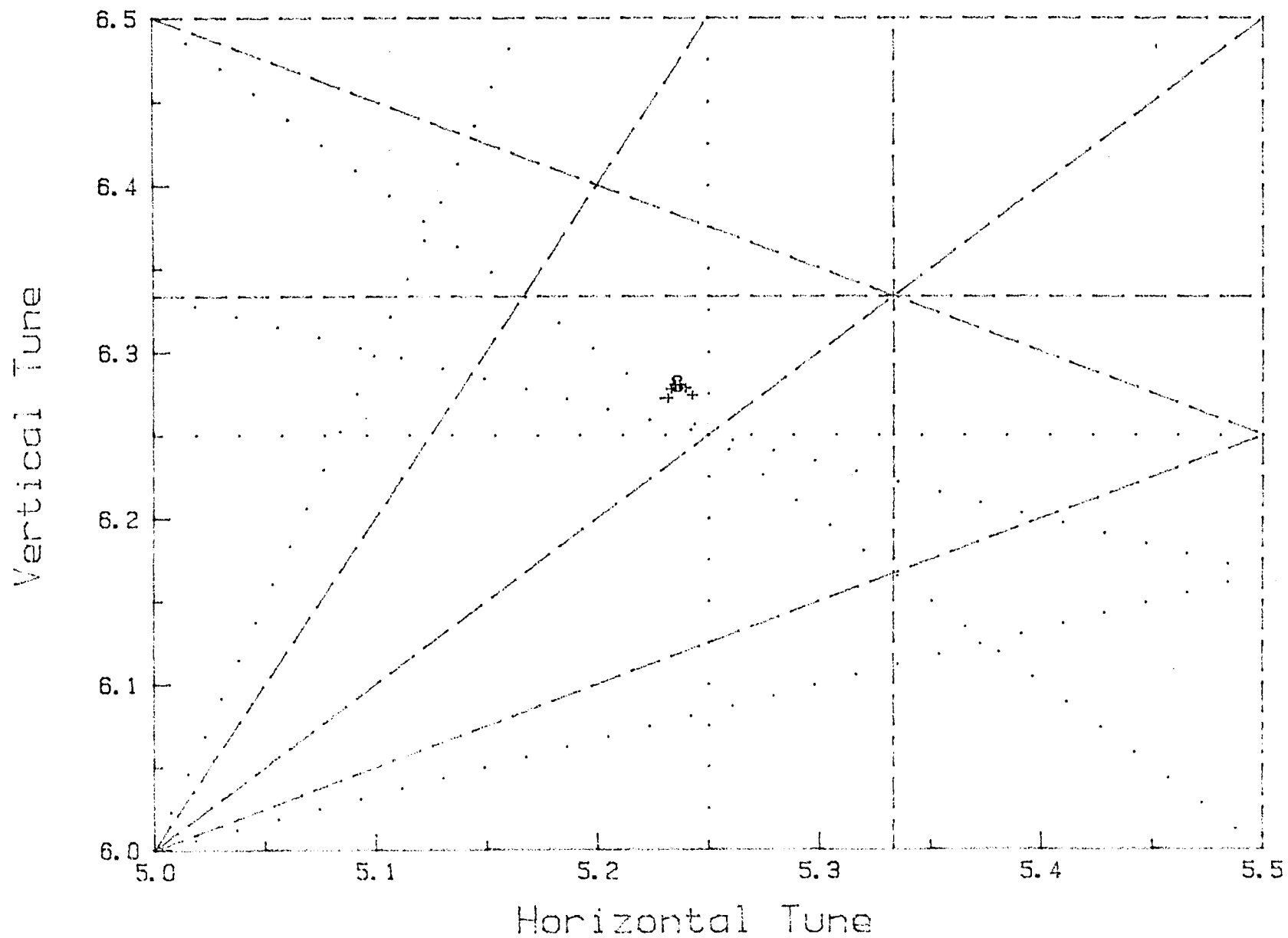


Figure 3(a). N30 Lattice Tune Diagram

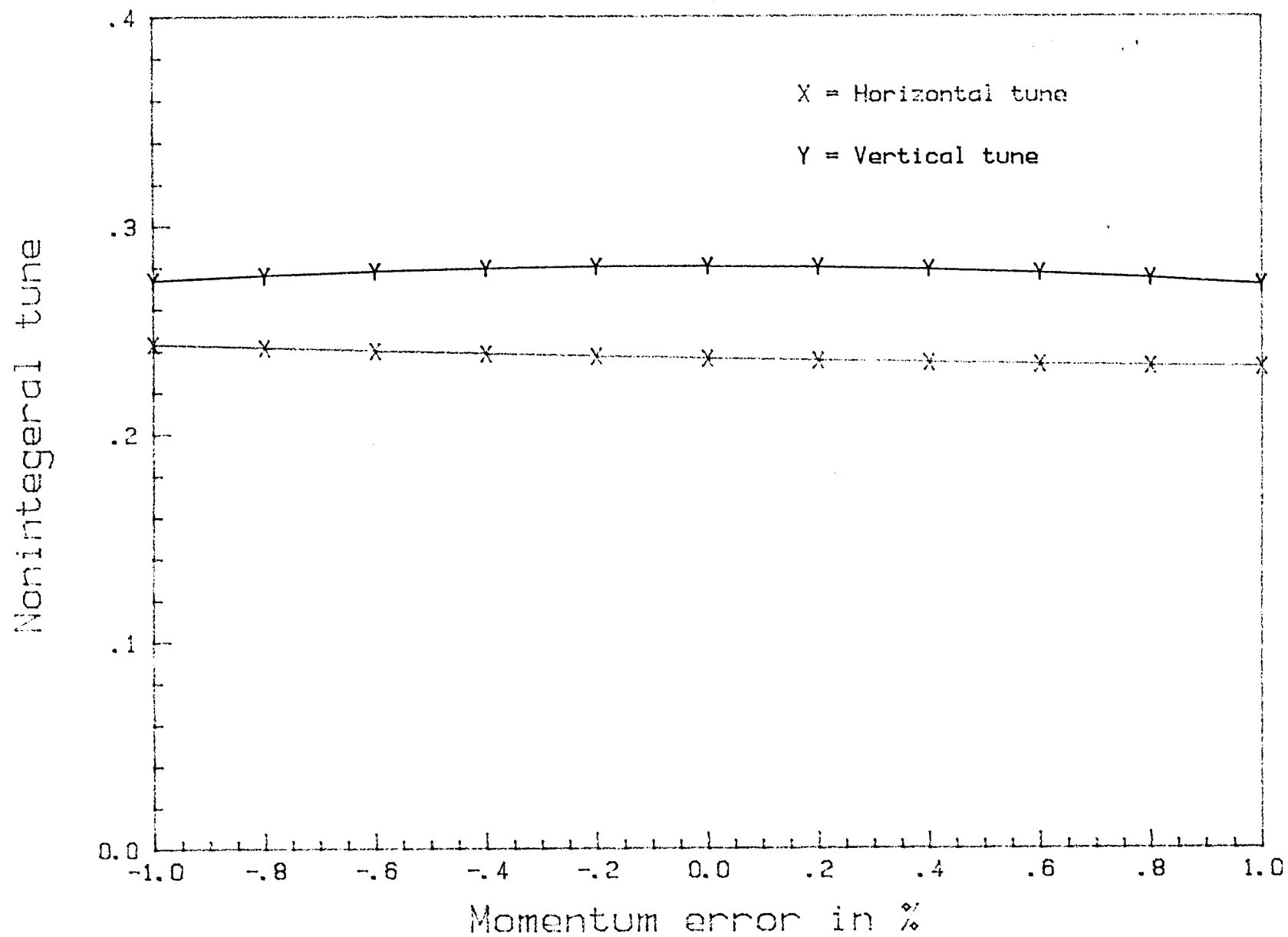


Figure 3(b). Tune Variation vs Momentum.

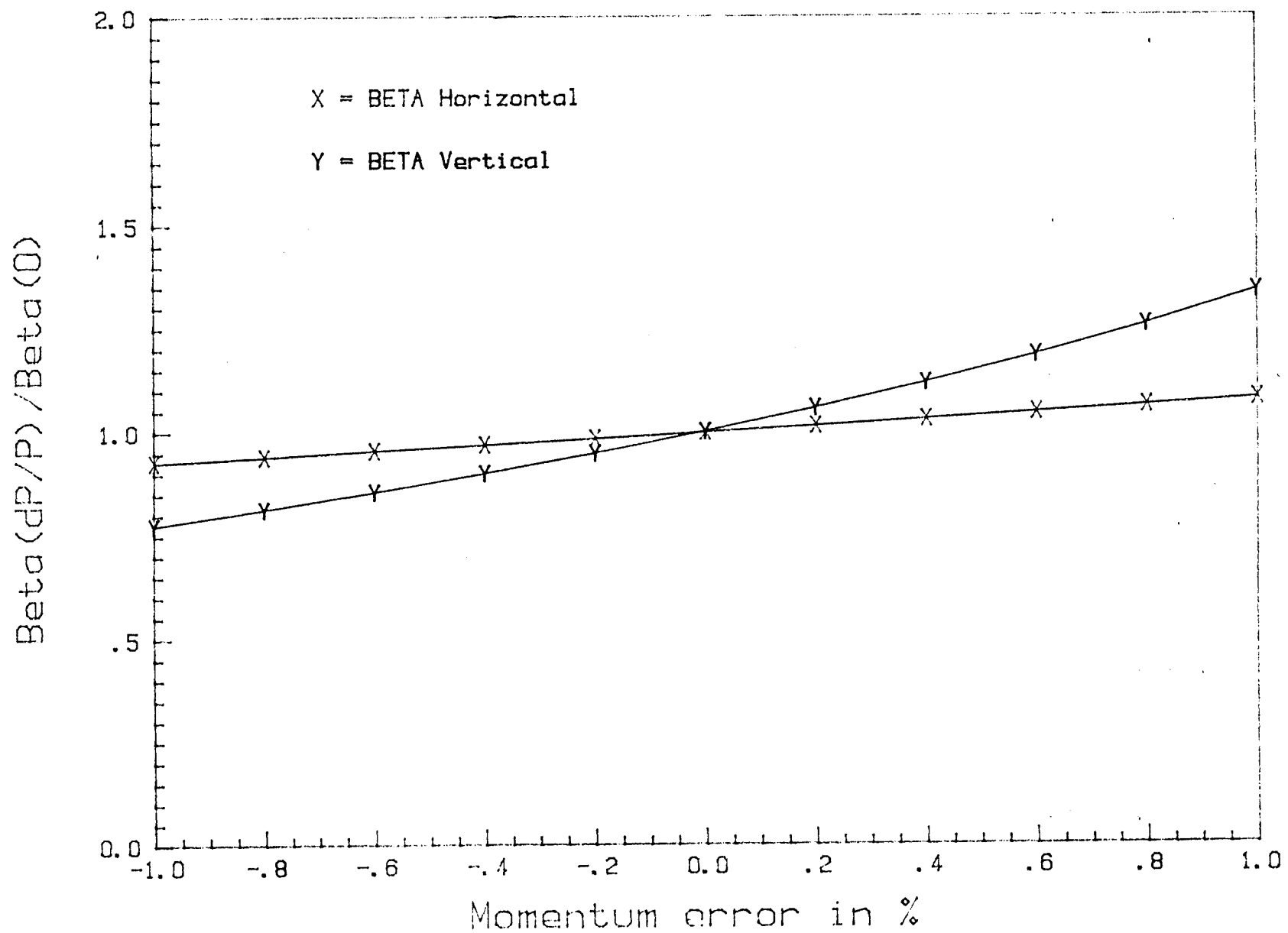


Figure 4(a). Ratio Beta vs Momentum.

$$\beta_y(\delta=1)/\beta_y(0)$$

$$\beta_x(\delta=1)/\beta_x(0)$$

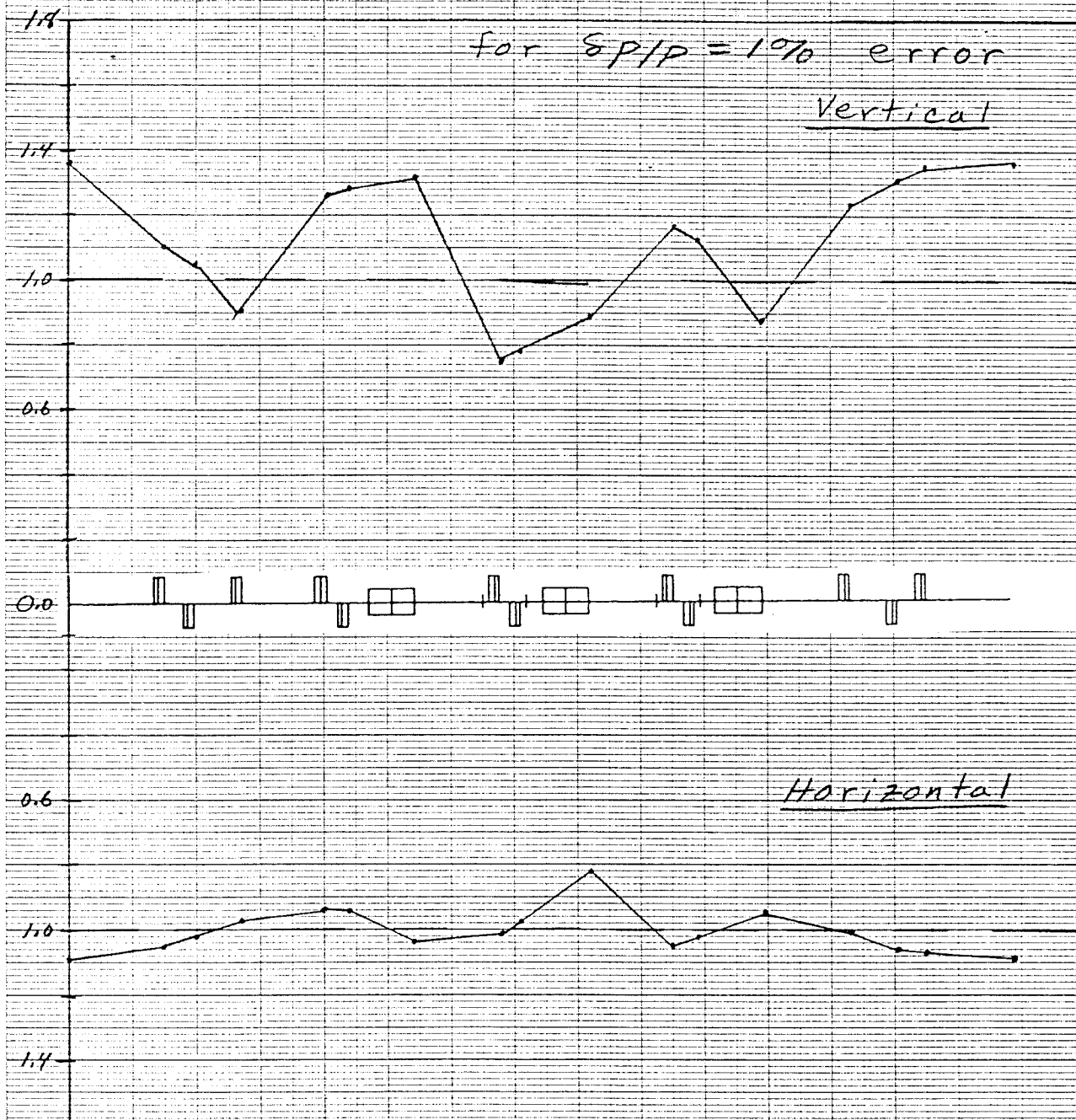


Figure 4(b). Beta Variation for N30 Lattice.

for  $\Delta\theta_{rms} = 0.1 \text{ mrad}$ , bend magnets  
 $\Delta X, Y_{rms} = 0.1 \text{ mm}$ , quadrupoles

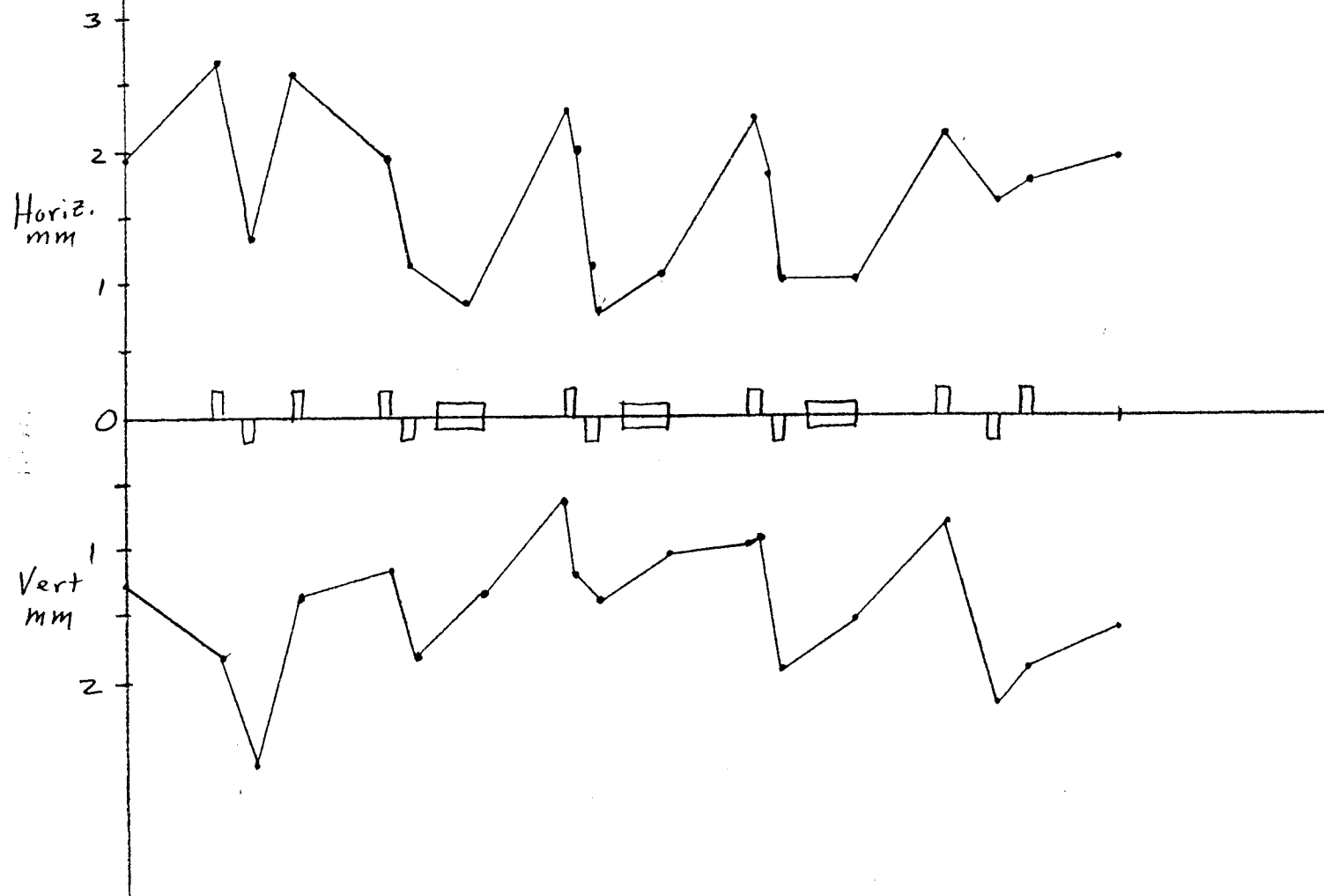


Figure 5. RMS Orbit Displacement for N30 Lattice.

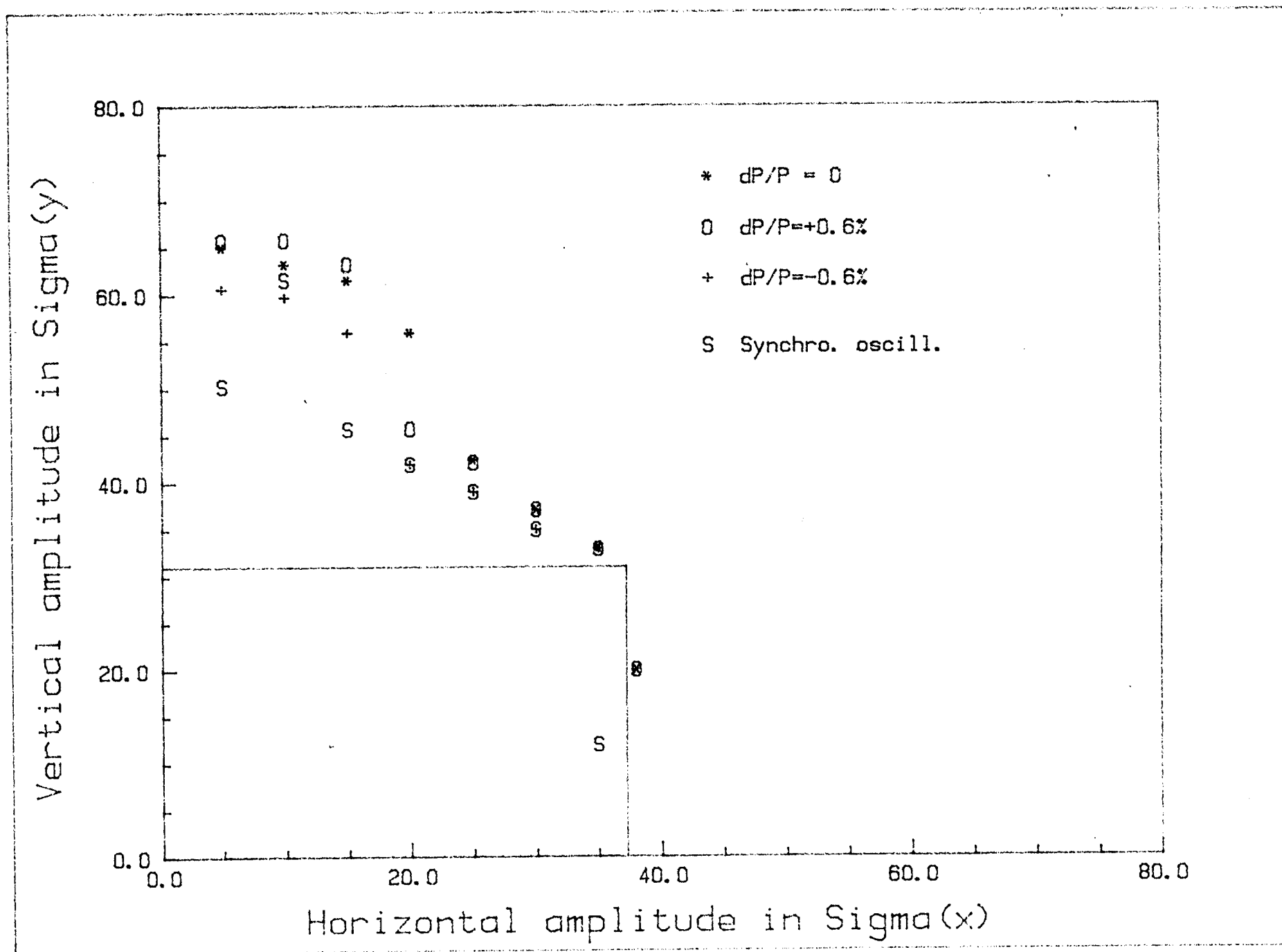
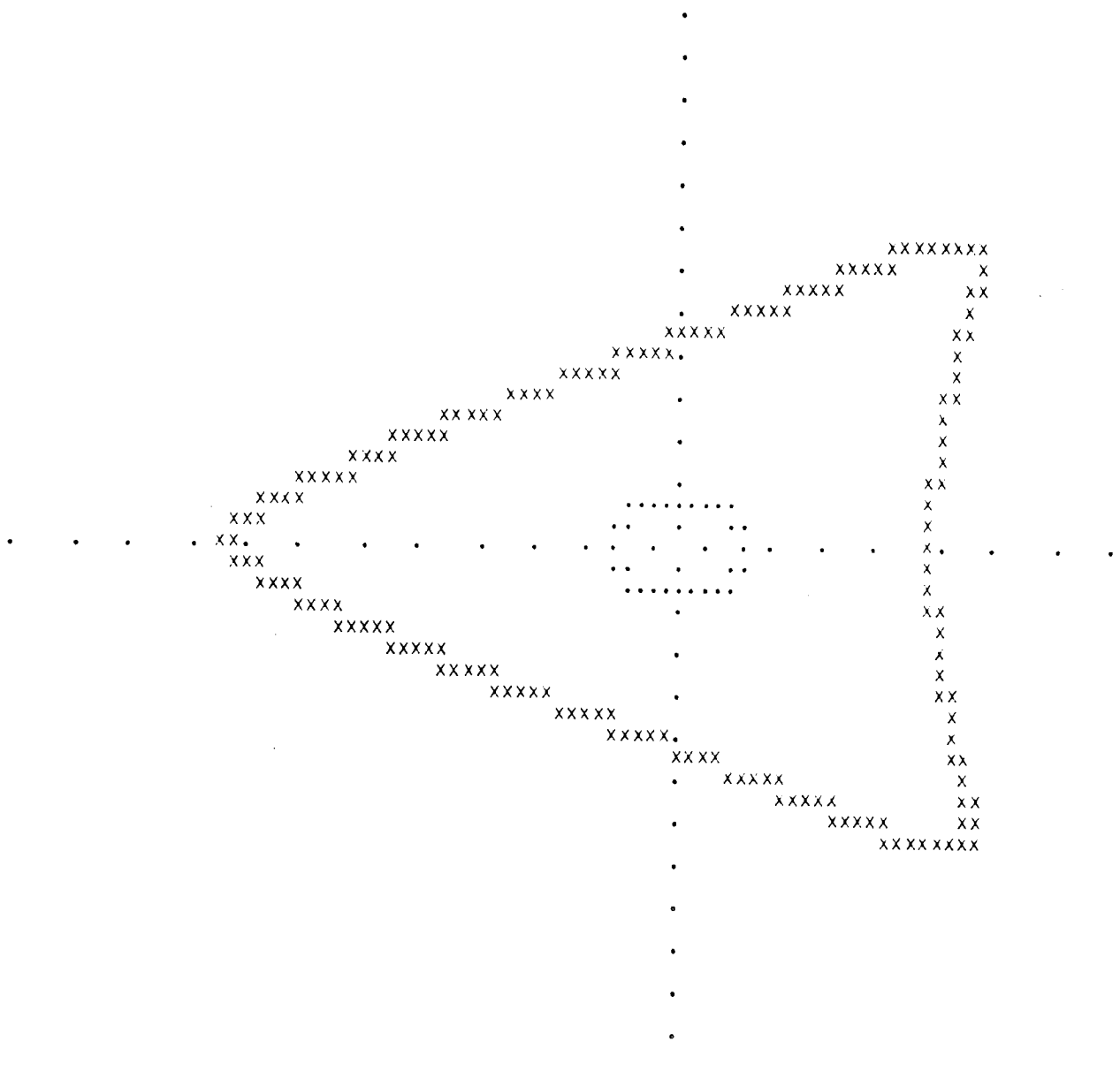


Figure 6. N30 Lattice Dynamic Aperture.

15.546	+	I
		I
		I
12.436	+	I
		I
		I
9.327	+	I
		I
		I
6.218	+	I
		I
		I
3.109	+	I
		I
		I
0.000	+	I
		I
		I
3.109	+	I
		I
		I
6.218	+	I
		I
		I
9.327	+	I
		I
		I
12.436	+	I
		I
		I
15.546	+	I



1  
45.12

\*\*\* PROGRAM 1

Figure 7. Particle Trajectory for  $N_x = 35$ ,  $N_y = 3.5$ .

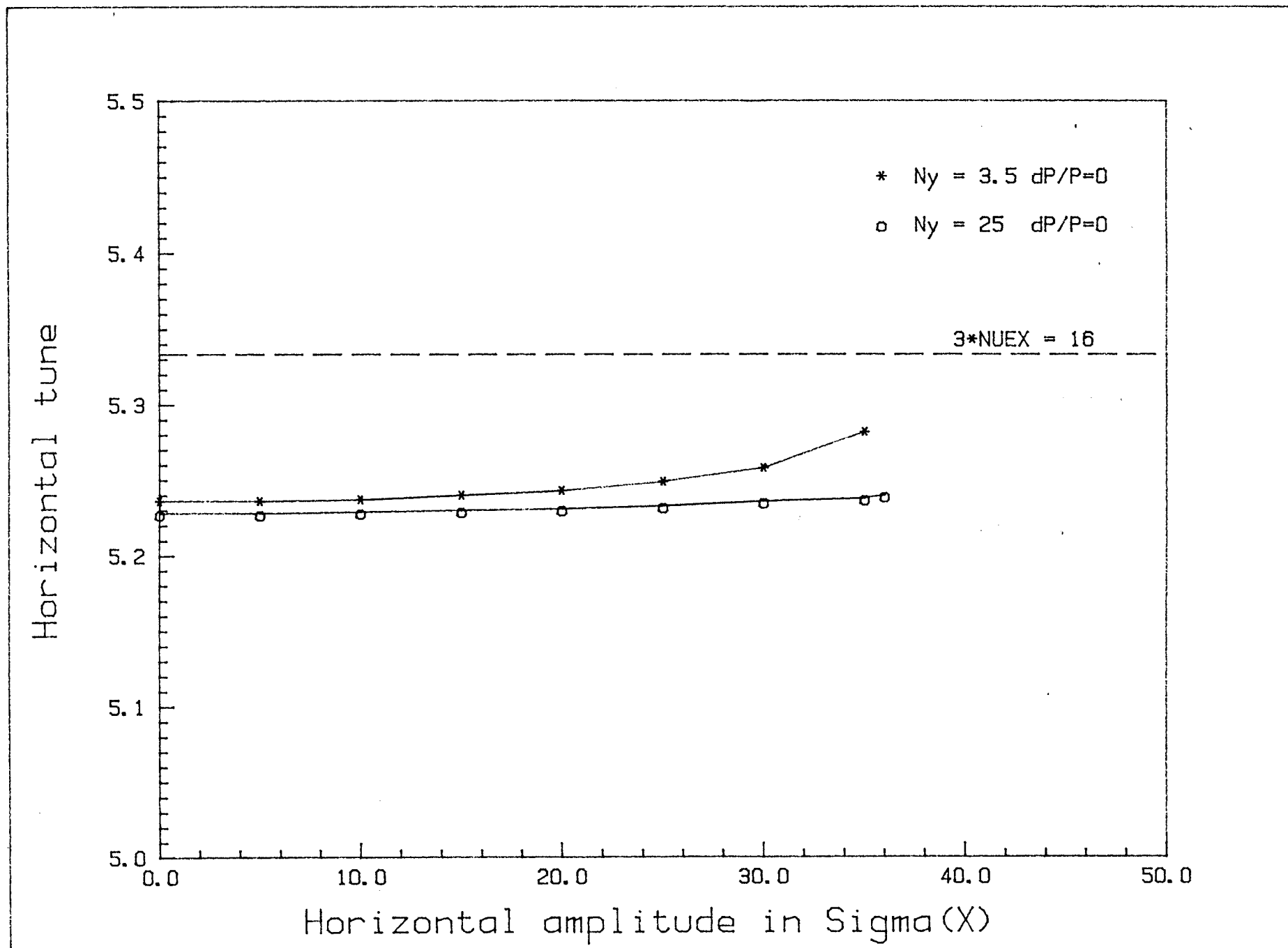


Figure 8. Tune vs Amplitude.



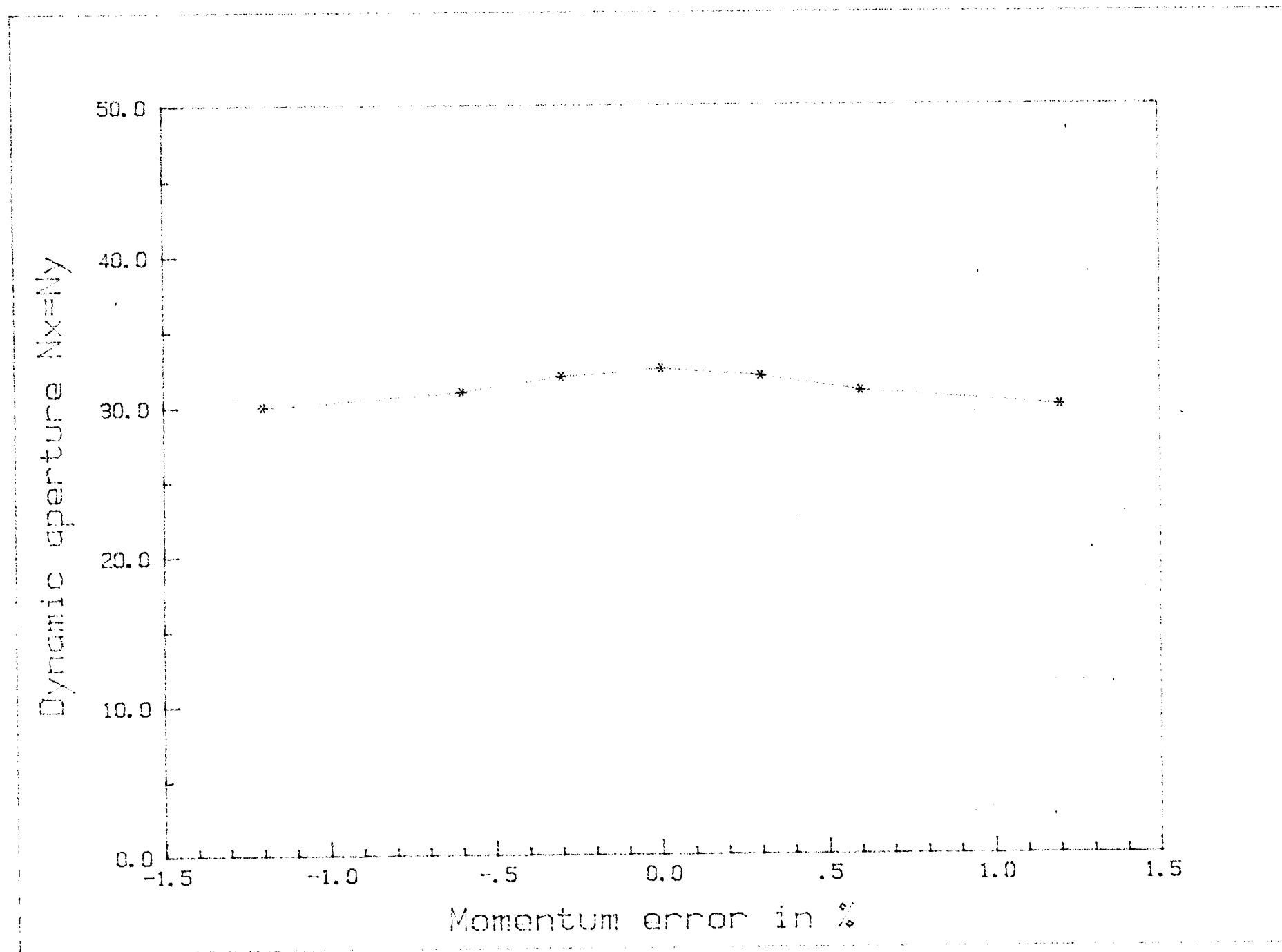


Figure 9. Aperture vs Momentum.